ACS APPLIED MATERIALS & INTERFACES

Research Article

www.acsami.org

Amide-Mediated Hydrogen Bonding at Organic Crystal/Water Interfaces Enables Selective Endotoxin Binding with Picomolar Affinity

Vincent Vagenende,* Tim-Jang Ching, Rui-Jing Chua, Navanita Thirumoorthi, and Pete Gagnon

Bioprocessing Technology Institute, A*STAR (Agency for Science, Technology and Research), 20 Biopolis Way #06-01 Centros, Singapore 138668

Supporting Information

ABSTRACT: Since the discovery of endotoxins as the primary toxic component of Gram-negative bacteria, researchers have pursued the quest for molecules that detect, neutralize, and remove endotoxins. Selective removal of endotoxins is particularly challenging for protein solutions and, to this day, no general method is available. Here, we report that crystals of the purine-derived compound allantoin selectively adsorb endotoxins with picomolar affinity through amide-mediated hydrogen bonding in aqueous solutions. Atom force microscopy and chemical inhibition experiments indicate that endotoxin adsorption is largely independent from hydrophobic and ionic interactions with allantoin crystals and is mediated by hydrogen bonding with amide groups at flat crystal surfaces. The small size (500 nm) and large specific surface area of allantoin crystals results in a very high endotoxin-binding capacity (3×10^7 EU/g) which compares favorably with known endotoxin-binding materials. These results provide a proof-of-concept for hydrogen bond-based molecular recognition processes in aqueous solutions and establish a practical method for removing endotoxins from protein solutions.

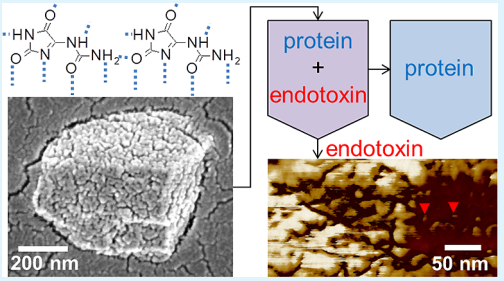

KEYWORDS: *hydrogen bonding, amide, endotoxin, organic crystals, purine, allantoin*

INTRODUCTION

Since the discovery of endotoxins as the primary toxic component of Gram-negative bacteria, researchers have pursued the quest for molecules that detect, neutralize, and remove endotoxins.[1−7] Selective removal of endotoxins is particularly challenging for protein solutions and, to this day, a general method for removing endotoxins from protein solutions is lacking.[8,9] Endotoxins are negatively charged lipopolysaccharides, and current methods for endotoxin removal from protein solutions mostly exploit ionic and/or hydrophobic interactions with endotoxin molecules.[8,9] While effective for certain proteins, these methods have several limitations. Methods using ion-exchange adsorbents[10−13] are sensitive to pH and salt concentration and are generally not suitable for acidic proteins.[8] Methods using hydrophobic adsorbents are less effective and are sensitive to salts and organic modifiers like solvents and detergents.[8] Biological affinity-based methods, which generally depend on a combination of ionic and hydrophobic interactions, may be robust over a wider range of conditions but generally impose high costs and risk of contamination by toxic affinity ligands.[8,14−18] Other endotoxin removal methods such as ultrafiltration and detergent-based extraction are generally not suitable for protein solutions due to their limited effectiveness, difficulty to remove residual detergents, and negative effects on protein stability and activity.[9]

Hydrogen bonding is a primary interaction force in nature where it conveys high selectivity to molecular recognition processes.[19−23] The contribution of hydrogen bonding to binding affinity is, however, solvent dependent and is generally very small in aqueous solution due to strong competition for hydrogen bonding by water.[24,25] For example, quadruple hydrogen-bonding arrays in organic solvents drive supramolecular assembly with high specificity and affinity,[26−31] whereas the stable assembly of complementary oligonucleotides in aqueous solution requires the association of at least four base pairs.[21,24] It is therefore not surprising that hydrogen-bond mediated supramolecular assembly in aqueous solutions is practically always supported by additional interactions involving charge or hydrophobicity. Even the extremely strong binding of complementary strands in the double DNA helix is primarily derived from aromatic stacking between adjacent bases rather than hydrogen bonding between complementary bases.[32] Using hydrogen bonding as the primary driving force for molecular recognition and supramolecular assembly in aqueous solutions therefore appears to be a considerable challenge.

We decided to explore the use of hydrogen bonding for selective endotoxin removal from protein solutions, and we pursued nonionic hydrophilic agents that might mediate

Received: March 20, 2013
Accepted: April 23, 2013
Published: April 23, 2013

selective binding of endotoxins with relatively minor protein binding. In particular, we focused on commercially available small molecule compounds that are poorly soluble in water. This led us to consider purine- and pyrimidine-based compounds, including the nucleobases of DNA. In this work, we report the discovery that undissolved particles of the purine-derived compound allantoin selectively remove more than 99.9% of endotoxins from protein solutions. We use dynamic light scattering, scanning electron microscopy, and atomic force microscopy to characterize endotoxin binding on allantoin particles, and we find that submicrometer allantoin crystals adsorb endotoxins with picomolar affinity. A series of inhibition assays with various organic and inorganic compounds confirms that endotoxin binding is largely independent from hydrophobic and ionic interactions with allantoin crystals and specifically depends on amide-mediated hydrogen bonding. The significance of these results is discussed within the context of materials that selectively bind endotoxins in aqueous solutions.

EXPERIMENTAL SECTION

Materials and Sample Preparation. Allantoin, 4-morpholineethanesulfonic acid (MES), 3-(cyclohexylamino)-2-hydroxy-1-propanesulfonic acid (CAPSO), guanidine hydrochloride (GdmCl), urea, sodium citrate, sodium dodecyl sulfate (SDS), γ-cyclodextrin, adenine, thymine, cytosine, guanine, uric acid, hydantoin, lysozyme, and bovine serum albumin (BSA) were purchased from Sigma-Aldrich. Sodium chloride (NaCl), 4-(2-hydroxyethyl)piperazine-1-ethanesulfonic acid (HEPES), citric acid, and ethanol were purchased from Merck Chemicals. Pluronic F68 was purchased from Gibco. Tween 20 was purchased from Promega. Diazolidinyl urea and biurea were purchased from Tokyo Chemical Industry.

Lipopolysaccharides (LPS) from *E. coli* O55:B5 purified by ion-exchange chromatography was purchased from Sigma-Aldrich. LPS was dissolved in endotoxin free water to a final concentration of 1 mg/mL and filtered with a 0.22 μm Millex-GV syringe filter unit (PVDF, 13 mm; Merck-Millipore). The LPS solution was subsequently diluted to 100 000 EU/mL by adding standard buffer (20 mM HEPES, 150 mM NaCl, pH 7.5). The diluted LPS solution was used for spiking at different endotoxin concentrations (10, 100, 1000, and 10 000 EU/mL, respectively). To investigate the effect of pH on endotoxin removal, LPS solutions were prepared in 20 mM citrate (pH 3.5), 20 mM MES (pH 5.5), and 20 mM CAPSO (pH 9.5), respectively.

Supernatant and cell lysate of an *E. coli* culture were obtained from a 1 L shake flask fermentation of *E. coli* BL21(DE3) cells. Cells were separated from the supernatant by centrifugation (4000*g*, 15 min), and the cell pellet was resuspended in 100 mL of 20 mM EDTA, 50 mM Tris (pH 7.8). The resuspended cells were lysed with a Microfluidizer (M-110P, Microfluidics) at 10 000 psi, and the lysate was centrifuged (17 000*g*, 15 min) to remove insoluble cell debris.

Endotoxin Removal by Purine- and Pyrimidine-Based Compounds. Endotoxin removal by the purine- and pyrimidine-based compounds guanine, cytosine, adenine, thymine, and allantoin was tested by adding the respective compounds to a protein solution (1 mg/mL BSA in 20 mM HEPES, pH 7.5, 150 mM NaCl, 1000 EU/mL) at a supersaturated concentration (300 mg/mL). Protein samples containing undissolved particles of the respective compounds were incubated on a rotary disc at 30 rpm for 15 min at room temperature. After incubation, undissolved particles were removed by centrifugation followed by filtration through a 0.22 μm filter. The endotoxin level of each sample was measured before adding the compound and after removal of undissolved particles, and endotoxin reduction factors were determined by dividing the respective values. Endotoxin concentrations were measured by a standard kinetic chromogenic Limulus Amebocyte Lysate (LAL) assay using LAL reagent (Endosafe Endochrome-K, Charles River Laboratories Inc.). Protein recovery was determined on the basis of protein peak area at $UV_{280\ nm}$ measured by size-exclusion chromatography on a Shimadzu Class-VP HPLC system with a TSK G3000SWxl column (Tosoh). Values of endotoxin removal and protein recovery reported in the study are the average of a minimum of two independent endotoxin removal experiments.

Endotoxin removal by allantoin was further characterized at different allantoin concentrations (4, 10, 50, 100, and 300 mg/mL) for protein solutions of lysozyme and BSA in the same way as described above. Endotoxin removal for *E. coli* culture supernatant and cell lysate was performed using 300 mg/mL allantoin in the same way as described above, and protein recoveries were analyzed on the basis of a standard Bradford protein assay (Thermo Scientific).

Endotoxin Binding Capacity and Affinity. Equilibrium data of endotoxin binding on undissolved allantoin were obtained by adding allantoin at 10, 50, 100, and 300 mg/mL to buffer (20 mM HEPES, 150 mM NaCl, pH 7.5) with endotoxin levels ranging from 10 to 10^6 EU/mL. Allantoin solutions were filtered, and endotoxin levels in the liquid phase (filtrate) were determined as described above. The corresponding endotoxin levels in undissolved allantoin were calculated from a mass balance. In this way, endotoxin binding equilibrium data were obtained over 8 orders of magnitude. The binding affinity and capacity for endotoxin binding by undissolved allantoin was determined by fitting experimental data to a 2-site Langmuir model as detailed in the Supporting Information.

Dynamic Light Scattering. Allantoin is supplied as a crystalline powder, and at concentrations above its solubility limit (~5 mg/mL), crystals in the allantoin powder persist in solution and a suspension of allantoin crystals is obtained. The size distribution of undissolved allantoin crystals was characterized by dynamic light scattering (DLS) on a light scattering photometer (Zetasizer Nano ZS; Malvern Instruments). Supersaturated allantoin (10 mg/mL) was placed in a 1 cm path-length quartz cuvette, and DLS measurements were carried out at room temperature. The hydrodynamic diameter was calculated by the Zetasizer software based on the Stokes–Einstein equation with a viscosity equal to that of water (0.8872 cP).

Scanning Electron Microscopy. The morphology of allantoin crystals was observed through a Jeol JSM-7600F field emission scanning electron microscope. To prepare samples, droplets of aqueous solutions of allantoin were air-dried and coated with gold using a Jeol JFC-1200 instrument. Although crystal sizes spanned a wide range (<1 μm to >10 μm), we found that the majority of crystals have dimensions of about 500 nm. No differences were observed between allantoin crystals with and without endotoxins.

Monolayer Endotoxin-Binding Capacity of Undissolved Allantoin. In this study, we found that undissolved allantoin exists as 500 nm crystals with evenly developed dimensions (see Results and Discussion). Assuming allantoin particles as 500 nm spheres and taking into account the density of allantoin (1.722 g/cm^3),[33] the specific area of undissolved allantoin was estimated to be ~7 m^2/g. Approximating an endotoxin molecule as a cylinder with a length of 9.6 nm and a diameter of 1.6 nm,[34] the surface area covered by a single endotoxin molecule was estimated to be ~15 nm^2. Accordingly, a monolayer of perfectly aligned endotoxin cylinders on the surface of allantoin particles was estimated to correspond with 0.7 μmol of endotoxin per gram of allantoin. Equating one endotoxin unit (1 EU) with 100 pg of endotoxin and considering that endotoxins have a molecular weight of 10–20 kDa[8], we further estimated that monolayer adsorption of endotoxins on allantoin crystals corresponds with ~30 to 80 million EU per gram of allantoin.

Atomic Force Microscopy. Atomic force microscopy (AFM) experiments were carried out using a Nanoscope V Dimension FastScan instrument (Bruker Inc.). Imaging in tapping mode was performed using a Fastscan-A silicon nitride cantilever with a spring constant of 18 N/m and a nominal tip radius of 5 nm. AFM scans were performed for allantoin crystals without endotoxins and for allantoin crystals saturated with endotoxins. Allantoin crystals saturated with endotoxins were obtained by adding an endotoxin amount exceeding the binding capacity of allantoin (i.e., 30 million EU per gram allantoin; see Results and Discussion) followed by a wash with an endotoxin-free saturated allantoin solution to remove unbound

endotoxin. Droplets of allantoin crystals in solution were applied on a glass slide and air-dried before AFM analysis.

RESULTS AND DISCUSSION

Selective endotoxin removal from a protein solution is tested for a number of purine- and pyrimidine-based compounds, including the nucleobases of DNA (Figure 1). The highest

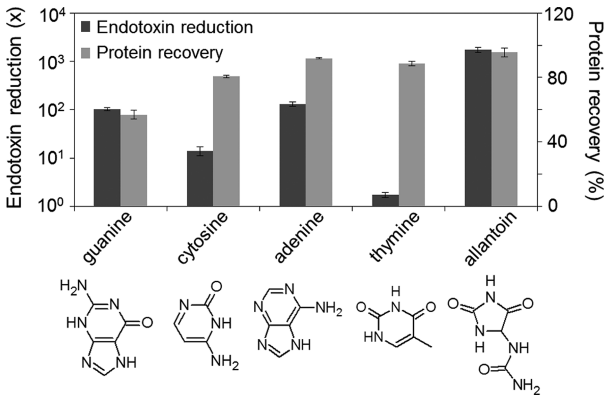

Figure 1. Endotoxin removal from protein solutions by purine- and pyrimidine-based compounds. Purine- and pyrimidine-based compounds were added to a protein solution (1 mg/mL BSA in 20 mM HEPES, pH 7.5, 150 mM NaCl with 1,000 EU/mL) at supersaturated concentrations (300 mg/mL) and undissolved particles were removed by filtration.

reduction of endotoxin levels (>99.9%) is observed for allantoin. Allantoin also compares favorably to the other compounds with respect to protein recovery (Figure 1). Following this encouraging result, endotoxin removal with allantoin is further investigated for BSA and lysozyme at various allantoin concentrations (Figure 2). Significant endotoxin reduction occurs for allantoin concentrations exceeding its solubility limit (~5 mg/mL), and endotoxin reduction factors continuously increase at higher allantoin concentrations (Figure 2a). Conversely, more than 80% of the proteins remain in solution for all allantoin concentrations tested (Figure 2b).

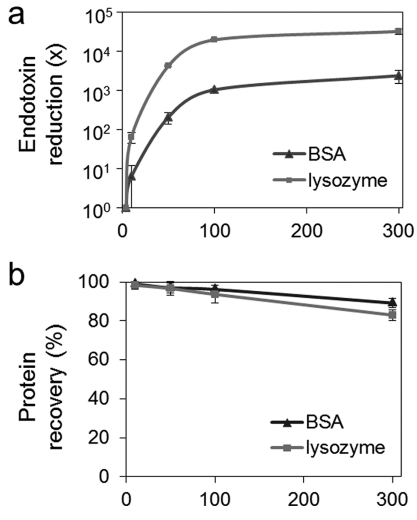

Figure 2. Effect of allantoin concentration on endotoxin removal by allantoin. The data show (a) endotoxin reduction and (b) protein recovery for lysozyme and BSA (1 mg/mL) in buffer (20 mM HEPES, pH 7.5, 150 mM NaCl) spiked with endotoxins (1000 EU/mL).

Good endotoxin removal with minimal protein loss is also observed for *E. coli* culture supernatant and cell lysate (Supplementary Table S1, Supporting Information). Addition and subsequent removal of undissolved allantoin thus appears an effective method for selective removal of endotoxins from protein solutions.

To gain insight in the mechanisms underlying endotoxin removal by undissolved allantoin, we characterize the distribution of endotoxins between aqueous solution and undissolved allantoin particles over a wide range of endotoxin concentrations (Figure 3a). An excellent fit is obtained over the entire concentration range using a 2-site Langmuir binding model for endotoxin adsorption at high affinity sites (H-sites) and ultrahigh affinity sites (U-sites) (Figure 3a). H-sites enable effective endotoxin-removal from low (<10 EU/mL) to very high (>10^6 EU/mL) endotoxin concentrations. U-sites enable further endotoxin reduction at low endotoxin concentrations (<10 EU/mL) due to their exceptionally high endotoxin binding affinity (K_a = 1 × 10^{10} M^{-1}). This endotoxin binding affinity is higher than for practically any other endotoxin-binding substance including antiendotoxic peptides,[3−6,35,36] endotoxin-binding proteins,[37−43] and engineered endotoxin-adsorbing materials.[44−47]

The size and morphology of undissolved allantoin particles are characterized by dynamic light scattering (DLS) and scanning electron microscopy (SEM). Analysis by DLS reveals a single peak at 500 nm corresponding with the mean diameter of allantoin particles (Figure 3b). Characterization by SEM shows that submicrometer allantoin particles have a crystalline morphology with evenly developed dimensions (Figure 3c). Taking into account the dimensions of an endotoxin molecule,[48] we estimate that a monolayer of endotoxin molecules on the surface of 500 nm spheres corresponds to 3 to 8 × 10^7 endotoxin units (EU) per gram of particles (see Experimental Section). This range quantitatively agrees with the endotoxin binding capacity of undissolved allantoin (3 × 10^7 EU/g), thereby suggesting that a major fraction of the surface of allantoin crystals is able to adsorb a layer of endotoxins. Furthermore, these results imply that the high endotoxin binding capacity of undissolved allantoin, which is several times higher than the endotoxin binding capacity of known endotoxin-binding adsorbents,[10,49−51] reflects the high specific surface area provided by submicrometer allantoin crystals.

Endotoxin adsorption on allantoin crystals is further characterized by atom force microscopy (AFM). In the absence of endotoxin, allantoin crystal surfaces appear flat with minimal phase contrast (Figure 4a,b and Supplementary Figure S1, Supporting Information). For allantoin crystals saturated with endotoxins, certain crystal planes appear completely covered with endotoxins, whereas other crystal planes are only partially covered (Figure 4c). Although several endotoxin molecules appear isolated on the crystal surface, most endotoxins form layer-like clusters comprising many endotoxin molecules (Figure 4d). The thickness of adsorbed endotoxin clusters is in the order of 5 nm (Supplementary Figure S1, Supporting Information), which corresponds with the molecular dimensions of an endotoxin molecule (~2−10 nm). This suggests endotoxin clusters consist of single- or double-layers of endotoxin molecules on the surface of allantoin crystals.

To probe the physicochemical interactions that drive the adsorption of endotoxins on allantoin crystals, we test endotoxin adsorption under various solution chemistry

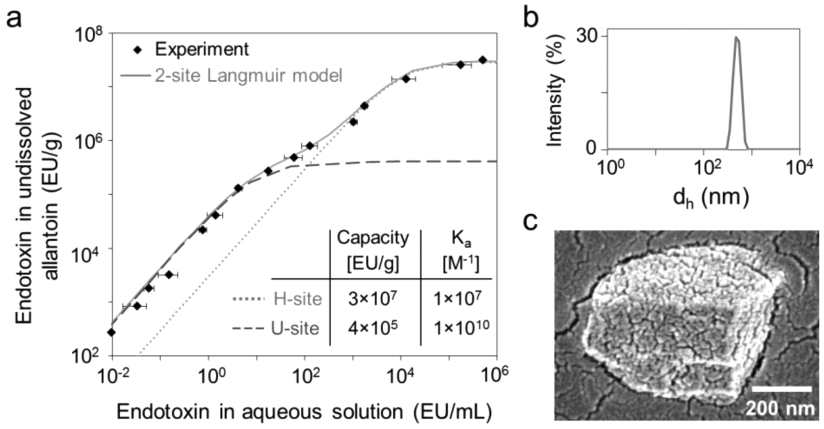

Figure 3. Undissolved allantoin exists as submicrometer crystals with high binding affinity and capacity for endotoxins. (a) Experimental data and 2-site Langmuir model fit for endotoxin distribution between aqueous solution and undissolved allantoin. (b) Hydrodynamic diameter of allantoin particles measured by dynamics light scattering (DLS). (c) SEM micrograph of a submicrometer allantoin crystal.

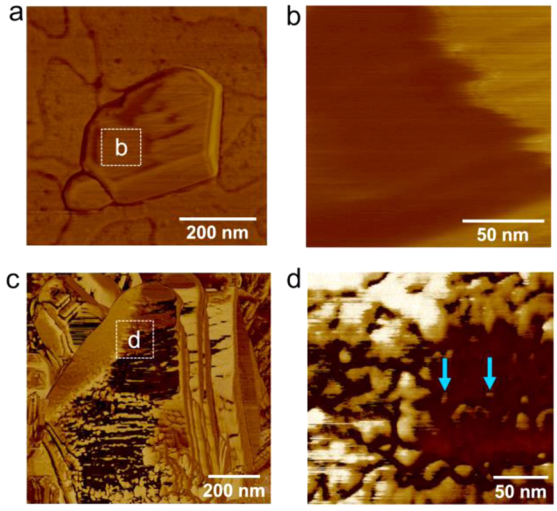

Figure 4. Phase contrast AFM images of allantoin crystals without endotoxin (a,b) and saturated with endotoxin (c,d). Blue arrows indicate single endotoxin molecules.

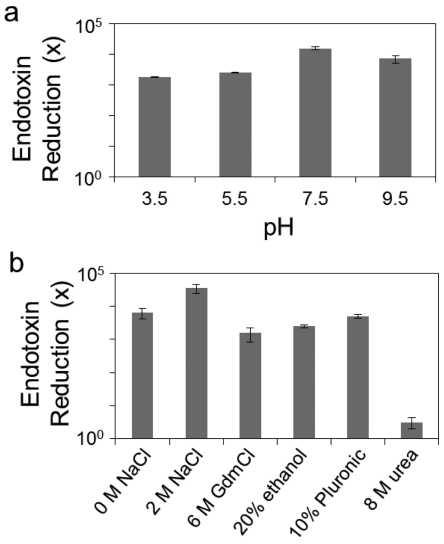

Figure 5. Endotoxin removal by allantoin under various solution chemistry conditions. Effects of pH (a) and various additives (b) on endotoxin removal by allantoin. All figures represent endotoxin reduction factors in aqueous solution (10 000 EU/mL) after treatment with 300 mg/mL allantoin.

conditions. Endotoxin removal by allantoin is effective over a broad pH range (Figure 5a), and the endotoxin removal efficiency increases in the presence of 2 M NaCl (Figure 5b). This indicates that endotoxin binding by allantoin does not depend on ionic interactions. Allantoin is also effective in removing endotoxins in the presence of guanidinium chloride, various organic solvents, and surfactants (Figure 5b and Supplementary Figure S2, Supporting Information). These results imply that endotoxin binding is largely independent from hydrophobic interactions with allantoin crystals. In contrast, practically no endotoxin removal occurs in the presence of 8 M urea (Figure 5b). Inhibition of endotoxin–allantoin binding by urea is concentration dependent and becomes maximal around 6 M urea (~30%) (Figure 6). Such concentration-dependent behavior is reminiscent of protein denaturation by urea, which involves the replacement of protein–protein and protein–water contacts by urea through relatively strong amide-mediated hydrogen bonding.[52,53] In the same way, urea is expected to inhibit endotoxin–allantoin binding by replacing hydrogen bonds between endotoxins and the amide groups of allantoin.

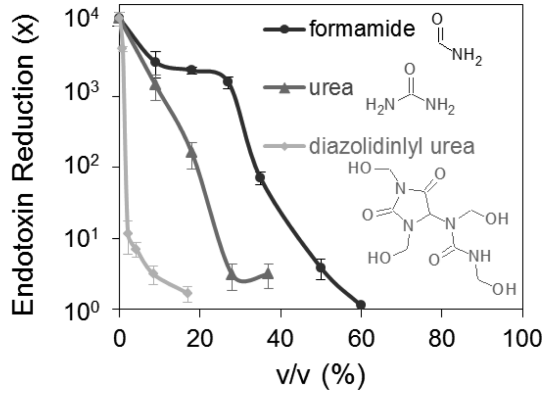

Figure 6. Chemical inhibition of endotoxin adsorption on allantoin crystals by soluble amide-based compounds. Graphs represent endotoxin reduction factors using 300 mg/mL allantoin from an aqueous solution (10 000 EU/mL) with formamide, urea, and diazolidinyl urea at the indicated concentrations.

dx.doi.org/10.1021/am401018q | ACS Appl. Mater. Interfaces 2013, 5, 4472–4478

Urea is twice as effective as formamide in inhibiting endotoxin binding by allantoin (Figure 6). Furthermore, inhibition experiments with the allantoin-derived compound diazolidinyl urea show minimal inhibition at ~1% but nearly complete inhibition at ~2% diazolidinyl urea (Figure 6). These data indicate that endotoxin binding by allantoin critically depends on the concentration of amide groups. Moreover, the strong increase of the inhibitory effect of diazolidinyl urea relative to urea indicates a strong correlation between the strength of molecular interactions and the number of amide groups per molecule. We propose therefore that the high endotoxin binding affinity of allantoin is the result of multivalent hydrogen bonding with amide groups on the surface of allantoin crystals.

We further examine the physicochemical origins of endotoxin removal by allantoin by comparing endotoxin removal by compounds that are structurally related to allantoin. Although allantoin consists of a hydantoin ring linked to urea, endotoxin removal by hydantoin and biurea is far less effective compared to allantoin (Figure 7). This discrepancy supports the

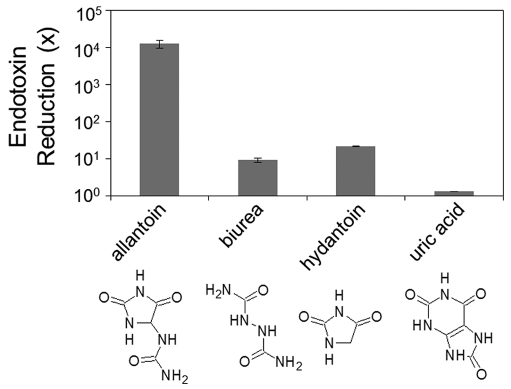

Figure 7. Comparison of endotoxin removal by compounds that are structurally related to allantoin. All compounds were used at 300 mg/mL, which is higher than the respective solubility limits.

proposition that endotoxin binding by allantoin crystals involves amide-mediated hydrogen bonding with both the hydantoin ring and the terminal urea group of allantoin. Another striking point is that practically no endotoxin removal occurs for the closely related compound uric acid (Figure 7). Unlike allantoin, bicyclic purine derivatives like uric acid have a planar structure which may complicate simultaneous intermolecular hydrogen bonding with amide groups in both purine rings. This structural difference is also reflected in the respective crystal structures: crystals of bicyclic purine derivatives consist of hydrogen-bonded sheets forming stacked arrays, whereas allantoin crystals consist of an intricate three-dimensional hydrogen-bond network.[33] The relative orientations of amide groups at the crystal/water interface of this three-dimensional hydrogen-bond network therefore appear essential for strong endotoxin binding through multivalent hydrogen bonding.

Selective binding of biomacromolecules on amide-rich surfaces has also been observed for molecular imprinted polymers (MIPs).[54,55] Unlike flat-surfaced allantoin crystals (Figure S1), MIPs bind their target molecules in complementary-shaped cavities, and hydrophobic and charged groups are commonly incorporated in the amide-based matrix to improve their selectivity and sensitivity. Nevertheless, binding affinities of MIPs are generally limited to the micromolar or nanomolar range,[56−59] and the practical use of MIPs for recognition of biomacromolecules remains extremely challenging.[60] Notably, a single study intended to fabricate an endotoxin-imprinted MIP using hydrophobic and charged groups.[61] Endotoxin binding by this MIP was only characterized for protein-free solutions and turned out to be more than 5 orders of magnitude weaker than endotoxin binding by allantoin crystals. This stark contrast corroborates the important role of the arrangement of amide groups for high-affinity endotoxin binding on allantoin crystals.

A variety of studies have focused on the adsorption of biomacromolecules on crystals in aqueous solutions.[62−65] The majority of these studies have been directed toward controlling crystal morphologies in biological systems,[66,67] and relatively little is known about the binding capacity and affinity of biomacromolecules on as-grown crystals. Addadi and coworkers showed that specific crystal surfaces can bind certain proteins: a phenomenon which was attributed to the stereochemical match between multiple crystal and protein functional groups.[62,63] Furthermore, the importance of steps on the crystal surface and the effects of surface chirality on protein adsorption have been highlighted.[65,68] Allantoin used in this study is a racemate, and we found that a major fraction of the flat surfaces of allantoin crystals adsorb endotoxins (Figure 4 and Supplementary Figure S1, Supporting Information). This suggests that crystal steps and surface chirality may not be essential for endotoxin binding on allantoin crystals.

Finally, we would like to point out that allantoin is generally regarded as a safe compound and its nontoxicity has been demonstrated by a large number of studies.[69] Allantoin is also a natural metabolite in human serum[70,71] and is widely used in various healthcare applications.[69,72] The presence of soluble allantoin after allantoin-based endotoxin removal is therefore not expected to be of concern for in vivo and cell-based protein applications. Besides, removal of soluble allantoin from protein solutions is readily achieved using standard buffer exchange techniques such as ultrafiltration (Supplementary Figure S3, Supporting Information). Allantoin-based endotoxin removal thus emerges as a practical method for removing endotoxins from protein solutions.

■ CONCLUSIONS

In summary, we have discovered that crystals of the purine-derived compound allantoin selectively adsorb endotoxins in aqueous protein solutions with picomolar affinity (K_a = 1 × 10^{10} M^{-1}). At concentrations above its solubility limit, undissolved allantoin exists as submicrometer crystals with even surfaces. Adsorption of endotoxin molecules results in layer-like clusters of endotoxin molecules that cover a major fraction of the crystal surface area upon saturation. Endotoxin adsorption on allantoin crystals is compatible with salts and hydrophobic compounds but is sensitive to amide-based compounds such as formamide and urea. Considering (1) the minimal role of ionic and hydrophobic interactions between allantoin crystals and endotoxins, (2) the inhibition of endotoxin adsorption by amide-containing compounds, which critically depends on the concentration and the number of amide groups per molecule, (3) urea's capacity for relatively strong hydrogen bonding in aqueous solutions, and (4) allantoin's diureide structure, which enables the formation of a three-dimensional hydrogen-bond network, we conclude that multivalent amide-mediated hydrogen bonding is the primary driving force for endotoxin adsorption on allantoin crystals in

aqueous solution. This study thus demonstrates the feasibility of using hydrogen bonding to drive molecular recognition in aqueous solutions and provides a practical method for removing endotoxins from protein solutions by exploiting the remarkable interface properties of allantoin crystals.

■ ASSOCIATED CONTENT

Supporting Information

Description of 2-site Langmuir model, AFM height images of allantoin particles, and effects of surfactants on the endotoxin removal efficiency by allantoin. This information is available free of charge via the Internet at http://pubs.acs.org.

■ AUTHOR INFORMATION

Corresponding Author

* E-mail: Vincent_Vagenende@bti.a-star.edu.sg.

Notes

The authors declare no competing financial interest.

■ ACKNOWLEDGMENTS

The authors would like to thank Lin Ming and Lai Mei Ying from the Institute of Materials Research and Engineering (A*STAR, Singapore) for assistance with the SEM experiments and Sun Wanxin and Wang Shu Rui from Bruker corporation for assistance with AFM experiments. This work was supported by the Biomedical Research Council of A*STAR (Agency for Science, Technology and Research), Singapore.

■ REFERENCES

(1) Beutler, B.; Rietschel, E. T. *Nat. Rev. Immunol.* **2003**, *3*, 169−176.
(2) Wu, J.; Zawistowski, A.; Ehrmann, M.; Yi, T.; Schmuck, C. *J. Am. Chem. Soc.* **2011**, *133*, 9720−9723.
(3) Bhattacharjya, S. *Curr. Med. Chem.* **2010**, *17*, 3080−3093.
(4) Brandenburg, K.; Andrae, J.; Garidel, P.; Gutsmann, T. *Appl. Microbiol. Biotechnol.* **2011**, *90*, 799−808.
(5) Rosenfeld, Y.; Sahl, H.-G.; Shai, Y. *Biochemistry* **2008**, *47*, 6468−6478.
(6) Tan, N. S.; Ng, M. L. P.; Yau, Y. H.; Chong, P. K. W.; Ho, B.; Ding, J. L. *FASEB J.* **2000**, *14*, 1801−1813.
(7) Riedemann, N. C.; Guo, R. F.; Ward, P. A. *Nat. Med.* **2003**, *9*, 517−524.
(8) Petsch, D.; Anspach, F. B. *J. Biotechnol.* **2000**, *76*, 97−119.
(9) Magalhaes, P. O.; Lopes, A. M.; Mazzola, P. G.; Rangel-Yagui, C.; Penna, T. C. V.; Pessoa, A. *J. Pharm. Pharm. Sci.* **2007**, *10*, 388−404.
(10) Chen, R. H.; Huang, C. J.; Newton, B. S.; Ritter, G.; Old, L. J.; Batt, C. A. *Protein Expression Purif.* **2009**, *64*, 76−81.
(11) Nian, R.; Chuah, C.; Lee, J.; Gan, H. T.; Latiff, S. M.; Lee, W. Y.; Vagenende, V.; Yang, Y. S.; Gagnon, P. *J. Chromatogr., A* **2013**, *1282*, 127−132.
(12) Guo, J.; Wei, Y.; Zhou, D.; Cai, P.; Jing, X.; Chen, X. S.; Huang, Y. *Biomacromolecules* **2011**, *12*, 737−746.
(13) Guo, J.; Meng, F.; Li, X.; Wang, M.; Wu, Y.; Jing, X.; Huang, Y. *Macromol. Biosci.* **2012**, *12*, 533−546.
(14) Kang, Y.; Luo, R. G. *Process Biochem.* **2000**, *36*, 85−92.
(15) Anspach, F. B. *J. Biochem. Biophys. Methods* **2001**, *49*, 665−681.
(16) Ding, J. L.; Zhu, Y.; Ho, B. *J. Chromatogr., B* **2001**, *759*, 237−246.
(17) Li, J.; Shang, G.; You, M.; Peng, S.; Wang, Z.; Wu, H.; Chen, G.-Q. *Biomacromolecules* **2011**, *12*, 602−608.
(18) Shimokawa, K. I.; Takakuwa, R.; Wada, Y.; Yamazaki, N.; Ishii, F. *Colloids Surf., B* **2013**, *101*, 350−352.
(19) Wilson, A. J. *Nat. Chem.* **2011**, *3*, 193−194.
(20) Bissantz, C.; Kuhn, B.; Stahl, M. *J. Med. Chem.* **2010**, *53*, 5061−5084.
(21) Philp, D.; Stoddart, J. F. *Angew. Chem., Int. Ed.* **1996**, *35*, 1155−1196.
(22) Fathalla, M.; Lawrence, C. M.; Zhang, N.; Sessler, J. L.; Jayawickramarajah, J. *Chem. Soc. Rev.* **2009**, *38*, 1608−1620.
(23) Sun, T.; Qing, G.; Su, B.; Jiang, L. *Chem. Soc. Rev.* **2011**, *40*, 2909−2921.
(24) Sawada, T.; Yoshizawa, M.; Sato, S.; Fujita, M. *Nat. Chem.* **2009**, *1*, 53−56.
(25) Ma, M.; Gong, Y.; Bong, D. *J. Am. Chem. Soc.* **2009**, *131*, 16919−16926.
(26) Sijbesma, R. P.; Beijer, F. H.; Brunsveld, L.; Folmer, B. J. B.; Hirschberg, J.; Lange, R. F. M.; Lowe, J. K. L.; Meijer, E. W. *Science* **1997**, *278*, 1601−1604.
(27) Park, T.; Zimmerman, S. C. *J. Am. Chem. Soc.* **2006**, *128*, 11582−11590.
(28) South, C. R.; Burd, C.; Weck, M. *Acc. Chem. Res.* **2007**, *40*, 63−74.
(29) de Greef, T. F. A.; Meijer, E. W. *Nature* **2008**, *453*, 171−173.
(30) Yashima, E.; Maeda, K.; Iida, H.; Furusho, Y.; Nagai, K. *Chem. Rev.* **2009**, *109*, 6102−6211.
(31) Safont-Sempere, M. M.; Fernandez, G.; Wuerthner, F. *Chem. Rev.* **2011**, *111*, 5784−5814.
(32) Yakovchuk, P.; Protozanova, E.; Frank-Kamenetskii, M. D. *Nucleic Acids Res.* **2006**, *34*, 564−574.
(33) Mootz, D. *Acta Crystallogr.* **1965**, *19*, 726−734.
(34) Kastowsky, M.; Gutberlet, T.; Bradaczek, H. *Eur. J. Biochem.* **1993**, *217*, 771−779.
(35) Ried, C.; Wahl, C.; Miethke, T.; Wellnhofer, G.; Landgraf, C.; Schneider Mergener, J.; Hoess, A. *J. Biol. Chem.* **1996**, *271*, 28120−28127.
(36) Vaara, M.; Viljanen, P. *Antimicrob. Agents Chemother.* **1985**, *27*, 548−554.
(37) Wood, D. M.; Parent, J. B.; Gazzano-Santoro, H.; Lim, E.; Pruyne, P. T.; Watkins, J. M.; Spoor, E. S.; Reardan, D. T.; Trown, P. W.; Conlon, P. J. *Circ. Shock* **1992**, *38*, 55−62.
(38) Gazzano-Santoro, H.; Meszaros, K.; Birr, C.; Carroll, S. F.; Theofan, G.; Horwitz, A. H.; Lim, E.; Aberle, S.; Kasler, H.; Parent, J. B. *Infect. Immun.* **1994**, *62*, 1185−1191.
(39) Mannon, B. A.; Kalatzis, E. S.; Weiss, J.; Elsbach, P. *J. Immunol.* **1989**, *142*, 2807−2812.
(40) Tobias, P. S.; Soldau, K.; Gegner, J. A.; Mintz, D.; Ulevitch, R. J. *J. Biol. Chem.* **1995**, *270*, 10482−10488.
(41) Han, J.; Mathison, J. C.; Ulevitch, R. J.; Tobias, P. S. *J. Biol. Chem.* **1994**, *269*, 8172−8175.
(42) Minetti, C. A. S. A.; Lin, Y.; Cislo, T.; Liu, T. Y. *J. Biol. Chem.* **1991**, *266*, 20773−20780.
(43) Akashi, S.; Saitoh, S.; Wakabayashi, Y.; Kikuchi, T.; Takamura, N.; Nagai, Y.; Kusumoto, Y.; Fukase, K.; Kusumoto, S.; Adachi, Y.; Kosugi, A.; Miyake, K. *J. Exp. Med.* **2003**, *198*, 1035−1042.
(44) Petsch, D.; Rantze, E.; Anspach, F. B. *J. Mol. Recognit.* **1998**, *11*, 222−230.
(45) Perianayagam, M. C.; Jaber, B. L. *Am. J. Nephrol.* **2008**, *28*, 802−807.
(46) Zhang, Y.; Yang, H.; Zhou, K.; Ping, Z. *React. Funct. Polym.* **2007**, *67*, 728−736.
(47) Li, J.; Zhang, Y.; Ping, Z.; Li, M.; Zhang, Q. *Process Biochem.* **2011**, *46*, 1462−1468.
(48) Kastowsky, M.; Gutberlet, T.; Bradaczek, H. *J. Bacteriol.* **1992**, *174*, 4798−4806.
(49) Bemberis, I.; Sakata, M.; Hirayama, C.; Kunitake, M.; Yamaguchi, Y.; Nakayama, M.; Todokoro, M. *Biopharm. Int.* **2005**, *18*, 50.
(50) Hanora, A.; Plieva, F. M.; Hedstrom, M.; Galaev, I. Y.; Mattiasson, B. *J. Biotechnol.* **2005**, *118*, 421−433.
(51) Zhang, J. P.; Wang, Q.; Smith, T. R.; Hurst, W. E.; Sulpizio, T. *Biotechnol. Prog.* **2005**, *21*, 1220−1225.
(52) Das, A.; Mukhopadhyay, C. *J. Phys. Chem. B* **2008**, *112*, 7903−7908.
(53) Guinn, E. J.; Pegram, L. M.; Capp, M. W.; Pollock, M. N.; Record, M. T., Jr. *Proc. Natl. Acad. Sci. U. S. A.* **2011**, *108*, 16932−16937.

(54) Bossi, A.; Bonini, F.; Turner, A. P. F.; Piletsky, S. A. *Biosens. Bioelectron.* **2007**, *22*, 1131−1137.
(55) Whitcombe, M. J.; Chianella, I.; Larcombe, L.; Piletsky, S. A.; Noble, J.; Porter, R.; Horgan, A. *Chem. Soc. Rev.* **2011**, *40*, 1547−1571.
(56) Haupt, K.; Mosbach, K. *Trends Biotechnol.* **1998**, *16*, 468−475.
(57) Chianella, I.; Lotierzo, M.; Piletsky, S. A.; Tothill, I. E.; Chen, B. N.; Karim, K.; Turner, A. P. F. *Anal. Chem.* **2002**, *74*, 1288−1293.
(58) Zeng, Z.; Hoshino, Y.; Rodriguez, A.; Yoo, H.; Shea, K. J. *ACS Nano* **2010**, *4*, 199−204.
(59) Tai, D.-F.; Jhang, M.-H.; Chen, G.-Y.; Wang, S.-C.; Lu, K.-H.; Lee, Y.-D.; Liu, H.-T. *Anal. Chem.* **2010**, *82*, 2290−2293.
(60) Verheyen, E.; Schillemans, J. P.; van Wijk, M.; Demeniex, M.-A.; Hennink, W. E.; van Nostrum, C. F. *Biomaterials* **2011**, *32*, 3008−3020.
(61) Ogawa, K.; Hyuga, M.; Okada, T.; Minoura, N. *Biosens. Bioelectron.* **2012**, *38*, 215−219.
(62) Addadi, L.; Weiner, S. *Proc. Natl. Acad. Sci. U. S. A.* **1985**, *82*, 4110−4114.
(63) Perl Treves, D.; Kessler, N.; Izhaky, D.; Addadi, L. *Chem. Biol.* **1996**, *3*, 567−577.
(64) Kurimoto, M.; Subramony, P.; Gurney, R. W.; Lovell, S.; Chmielewski, J.; Kahr, B. *J. Am. Chem. Soc.* **1999**, *121*, 6952−6953.
(65) Kahr, B.; Gurney, R. W. *Chem. Rev.* **2001**, *101*, 893−951.
(66) Meldrum, F. C.; Coelfen, H. *Chem. Rev.* **2008**, *108*, 4332−4432.
(67) Nudelman, F.; Sommerdijk, N. A. J. M. *Angew. Chem., Int. Ed.* **2012**, *51*, 6582−6596.
(68) Zhang, M.; Qing, G.; Sun, T. *Chem. Soc. Rev.* **2012**, *41*, 1972−1984.
(69) Becker, L. C.; Bergfeld, W. F.; Belsito, D. V.; Klaassen, C. D.; Marks, J. G., Jr.; Shank, R. C.; Slaga, T. J.; Snyder, P. W.; Andersen, F. A. *Int. J. Toxicol.* **2010**, *29*, 84S−97S.
(70) Gruber, J.; Tang, S. Y.; Jenner, A. M.; Mudway, I.; Blomberg, A.; Behndig, A.; Kasiman, K.; Lee, C.-Y. J.; Seet, R. C. S.; Zhang, W.; Chen, C.; Kelly, F. J.; Halliwell, B. *Antioxid. Redox Signaling* **2009**, *11*, 1767−1776.
(71) Benzie, I. F. F.; Chung, W. Y.; Tomlinson, B. *Clin. Chem.* **1999**, *45*, 901−904.
(72) Araujo, L. U.; Grabe-Guimaraes, A.; Furtado Mosqueira, V. C.; Carneiro, C. M.; Silva-Barcellos, N. M. *Acta Cirurgica Bras.* **2010**, *25*, 460−466.